The Interaction of an Eastward-Flowing Current and an Island: Sub- and Supercritical Flow

JOSEPH PEDLOSKY AND MICHAEL A. SPALL

Woods Hole Oceanographic Institution, Woods Hole, Massachusetts

(Manuscript received 31 March 2015, in final form 25 August 2015)

ABSTRACT

An eastward-flowing current of a homogeneous fluid with velocity U, contained in a channel of width L, impinges on an island of width of $O(L)$, and the resulting interaction and dynamics are studied for values of the supercriticality parameter, $b = \beta L^2/U$, both larger and smaller than π^2. The former case is subcritical with respect to Rossby waves, and the latter is supercritical. The nature of the flow field depends strongly on b, and in particular, the nature of the flow around the island and the proportion of the flow passing to the north or south of the island are sensitive to b and to the position of the island in the channel. The problem is studied analytically in a relatively simple, nonlinear quasigeostrophic and adiabatic framework and numerically with a shallow-water model that allows a qualitative extension of the results to the equator. Although the issues involved are motivated by the interaction of the Equatorial Undercurrent and the Galapagos Islands, the analysis presented here focuses on the fundamental issue of the distinctive nature of the flow as a function of Rossby wave criticality.

1. Introduction

The Equatorial Undercurrent (EUC) in the Pacific runs eastward unimpeded until encountering the Galapagos Islands, which straddle the equator near 90°W. Numerical models, for example, Karnauskas et al. (2007), suggest that the interaction with the island diverts the flow, somewhat weakens it, and has a notable influence on the thermal structure of the eastern equatorial Pacific. The fact that the impinging flow is eastward raises the possibility of a wave response to the current–island interaction. The focus of the present paper is the extensive nature of the wave response and how it may affect the manner in which the current navigates a path around the island obstacle and its effect on the more distant flow. An interesting observational study by Karnauskas et al. (2010) concentrates on the near field around the island and so sheds little light on the possibility of a spatially extensive response.

To simplify the essential aspects of the problem as much as possible, we move the current off the equator in order to initially avoid the complexities of equatorial dynamics so that we can focus on issues associated with the super- or subcriticality of the flow, defined in the following section, with respect to Rossby waves. This simplifies both the analytical and numerical treatments of the problem. After a discussion of that simplified problem, we will demonstrate the pertinence of those results to the equatorial problem, albeit in a model that is suggestive, although less than fully realistic.

The scaling for an inertial EUC (Charney 1960; Pedlosky 1987a) implies that the current's lateral extent is on the order of $\delta_I = (U/\beta)^{1/2}$, where U is the characteristic current speed and β is the planetary vorticity gradient. We will replace the equatorial confinement mechanism with a simple channel of width L of a width comparable to δ_I and, at first, use quasigeostrophic dynamics to develop a theoretical understanding of the island–current interaction. These basic predictions are then largely supported with a shallow-water numerical model. The important point is that the above scaling is also equivalent to the condition of near criticality with respect to long, stationary Rossby waves in the current, more precisely whether $b = \beta L^2/U$ is greater or less than π^2. We are then in a position to examine the important dynamical nature of the interaction in a framework much simpler than the equatorial variant of the same

Corresponding author address: Joseph Pedlosky, Woods Hole Oceanographic Institution, 266 Woods Hole Rd., MS 21, Woods Hole, MA 02543.
E-mail: jpedlosky@whoi.edu

DOI: 10.1175/JPO-D-15-0061.1

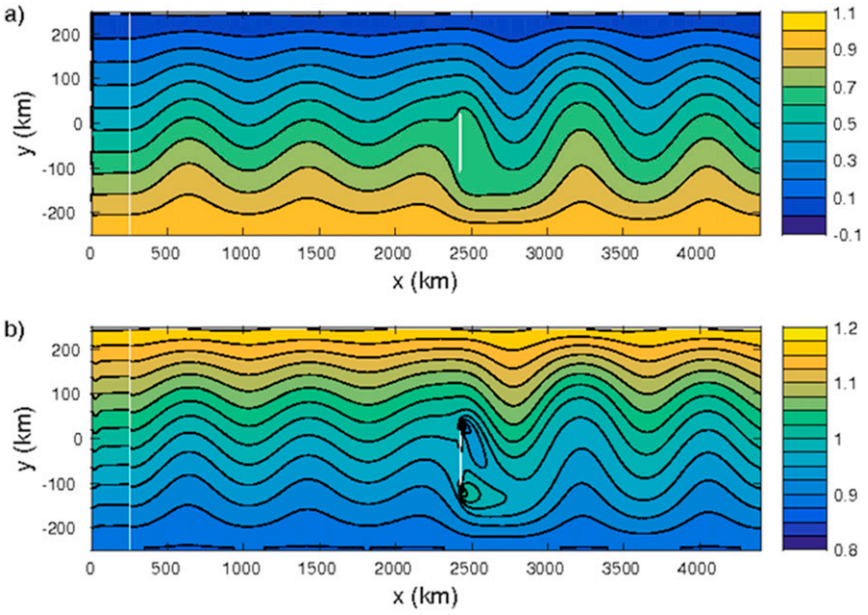

FIG. 1. An example showing a subcritical flow past an island obstacle illustrating the global wave response. (top) The streamfunction and (bottom) the potential vorticity. For this numerical calculation, U is 0.2 m s^{-1}, $b = 2.5\pi^2$, and the horizontal viscosity A_h is 500 m^2 s^{-1}. The center of the island is slightly below the midpoint of the channel allowing the excitation of the first Rossby mode.

problem. In particular, it allows a relatively simple solution for the steady, nonlinear problem for both supercritical and subcritical flows, that is, when b/π^2 is less or greater than unity but always of order one.

The problem of an eastward flow past an obstacle on the beta plane has a long and rich history, for example, Page and Johnson (1990) and Tansley and Marshall (2001); the latter reference in particular provides a valuable review of previous work. Most of that previous work has concentrated on the nature of the flow near the island obstacle, with a focus on the occurrence of separation of the flow around the island, using the Reynolds number, a measure of the importance of lateral friction with respect to inertia, as a control parameter. Although the Reynolds number can never be neglected completely when discussing flow past solid bodies, in this study we are concerned with a particularly global aspect of the flow, for example, the wave field generated by the obstacle in the subcritical case and its consequences for the island and will consider largely inviscid flows, and so the Reynolds number is less pertinent. As mentioned above, our interest is in the parameter b of order unity.

By way of motivation, we show in Fig. 1 the result of a numerical calculation using a shallow-water model on a beta plane with uniform inflow and outflow of 0.2 m s^{-1} (details of the model are given in section 5). In this case, $b = 2.5\pi^2$, which is in the subcritical regime and demonstrates an example of a global, steady, wavelike response. Small regions of anomalous potential vorticity are also seen in the island wake, but they are confined to the near-island region and, it will be demonstrated below, are not involved with the global wavelike response.

In an attempt to clarify the nature of the basic dynamics, we will first discuss an analytic model in section 2 based on potential vorticity conservation and formulate its general analytical solution. In section 3, we discuss in detail the supercritical case $b < 1$, while section 4 discusses the subcritical case. Section 5 describes our numerical approach to the problem, which also serves to suggest that our results are pertinent to the equatorial case. The results are summarized in section 6.

2. The theoretical model

a. Governing equations

The motion to be studied analytically is governed by the frictionless, adiabatic, quasigeostrophic equations (Pedlosky 1987b) for the geostrophic streamfunction ψ. In section 5, the effects of friction are addressed numerically. For lengths scaled with the channel width L, velocities with the characteristic velocity U, and time with the advective scale L/U, the governing equation is

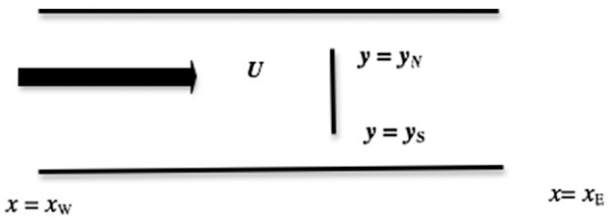

FIG. 2. A schematic of the problem domain. A channel of width L has a current U, entering at its western boundary x_w. It impinges on a thin island at $x = 0$ oriented meridionally between latitudes y_s and y_n. Gaps between the ends of the islands and the channel boundaries allow flow around the island.

$$\frac{\partial q}{\partial t} + J(\psi, q) + b\frac{\partial \psi}{\partial x} = 0, \quad q = \nabla^2\psi - F\psi, \quad b = (\beta L^2/U). \tag{2.1a,b,c}$$

Here, $J(\psi, q)$ is the Jacobian of the geostrophic streamfunction ψ and potential vorticity q with respect to x and y, the former as the downstream variable and the latter as the cross-stream variable, and the Laplacian is with respect to those two coordinates. The motion is restricted to an upper layer of depth H; the reduced gravity is g'. The Coriolis parameter at the southern boundary of the channel is f_0, and the planetary vorticity gradient is β. The flow, as shown in Fig. 2, enters the channel at $x = x_w < 0$ and exits at $x = x_e > 0$. The island is placed at $x = 0$ and is represented as a thin meridional line segment.

For a single layer of constant density fluid, F would be the square of the channel width to the external deformation radius, that is, $F = (f_0^2 L^2)/(gH)$. For the same layer over an infinitely deep layer of slightly denser fluid, it would be the square of the channel width to the internal deformation radius so that g is replaced by g', the reduced gravity. Since the theory to be described is applied to a steady state, the parameter F drops out of the problem. The speed of Rossby waves with x wavenumber k and cross-channel mode number $j\pi$ becomes stationary for either model when $b = k^2 + j^2\pi^2$, $j = 1, 2, 3, \ldots$, so that the minimum value of b necessary for the existence of a steady wave solution corresponds to $j = 1$, $k = 0$, for which $b = \pi^2$, which is the critical value separating sub- and supercritical currents.

For steady flow, the general solution of the potential vorticity equation [(2.1a)] is

$$\nabla^2\psi + b\psi = Q(\psi), \tag{2.2}$$

where $Q(\psi)$ is an arbitrary function of ψ.

At the western entrance to the channel, $x = x_w < 0$ the flow will be specified to be constant in time, independent of the cross-channel coordinate y, and possess no relative vorticity. Hence, at the entrance, $\psi = -y$ and $\nabla^2\psi = 0$. It follows that at the entrance $Q(\psi) = by = -b\psi$. This relationship is preserved on all streamlines issuing from the entrance. Thus, for all such streamlines, (2.2) becomes

$$\nabla^2\psi + b\psi = -by. \tag{2.3}$$

The boundary conditions at the channel walls are that the cross-channel velocity $v = \partial\psi/\partial x$ vanishes; hence,

$$\frac{\partial}{\partial x}\psi = 0, \quad y = 0, 1. \tag{2.4}$$

It is convenient to write ψ as

$$\psi = -y + \varphi(x, y). \tag{2.5}$$

The boundary conditions on φ are

$$\varphi = \begin{cases} 0, & y = 0, 1 \\ 0, & x = x_w \\ \Phi(y) & x = x_e \end{cases}. \tag{2.6a,b,c}$$

The first condition from (2.6a) ensures that the total transport eastward remains fixed, (2.6b) fixes the entering flow to be independent of y and, by (2.3), has zero relative vorticity upon entering. The last boundary condition allows us to fix, with an appropriate choice of Φ, the exiting flow velocity at the eastern end of the channel to insure that as much flow leaves the channel as enters. In setting the exit velocity to be a function of y, we are attempting to model the equivalent of the efflux of fluid at the eastern boundary into currents that carry the exiting fluid to the north or south along the eastern boundary just as the boundary condition at the western boundary is a simple model of fluid exiting from a western boundary current. The conditions we impose are a simplification of that situation that is convenient for our calculation. We emphasize that this condition at the eastern boundary, which qualitatively reflects the effect of an impermeable oceanic eastern wall, differs from the condition applied by Tansley and Marshall (2001), who allow the flow to exit into a damped region, which is the same approach as used below in section 5. Note that as a consequence, for steady flow, the governing equation [(2.3)] is an elliptic partial differential equation requiring boundary conditions on the streamfunction at all boundaries, entrance as well as exit. The streamfunction for the analytic model varies from −1 to 0 on inflow, while for the numerical model it varies from 0 to 1. This offset has no influence on the circulation or interpretation.

b. General solution

The general solution for φ can be written as a sine series in y:

$$\varphi = \sum_{j=1}^{J_{\max}} \varphi_j(x) \sin j\pi y, \tag{2.7}$$

where $J_{\max}$ is the last term kept in what is, in principle, an infinite series.

It follows that φ_j satisfies

$$\frac{\partial^2 \varphi}{\partial x^2} + (b - j^2\pi^2)\varphi = 0. \tag{2.8}$$

For values of j such that $b > j^2\pi^2$, the solution will be wavelike in x. For higher values of j, the solution will have an exponential character.

Let J_w be the largest value of j for which $b > j^2\pi^2$. Then, for $x_w \le x \le 0$, that is, west of the island, the solution to (2.8) can be written as

$$\varphi = \sum_{j=1}^{J_w} (A_j^- \cos k_j x + B_j^- \sin k_j x) \sin j\pi y + \sum_{j=J_w+1}^{J_{\max}} C_j^- e^{\alpha_j x} \sin j\pi y. \tag{2.9a}$$

In (2.9), it is assumed that the island is sufficiently distant from the entrance so that the exponential terms in (2.9a) are negligibly small at the entrance.

For $0 \le x \le x_e$, the general solution is given by

$$\varphi = \sum_{j=1}^{J_w} (A_j^+ \cos k_j x + B_j^+ \sin k_j x) \sin j\pi y + \sum_{j=J_w+1}^{J_{\max}} [C_j^+ e^{-\alpha_j x} + E_j e^{-\alpha_j (x_e - x)}] \sin j\pi y. \tag{2.9b}$$

In each of (2.9a) and (2.9b),

$$k_j = (b - j^2\pi^2)^{1/2} \quad b > j^2\pi^2$$
$$\alpha_j = (j^2\pi^2 - b)^{1/2} \quad b < j^2\pi^2. \tag{2.10a,b}$$

In (2.9b), it is assumed that $\alpha_j x_e$ is large enough so that the contribution it makes to the solution is small everywhere except near the eastern boundary where it is used to satisfy (2.6c).

The coefficients in the solution are determined from the conditions (2.6a), (2.6b), and (2.6c) and the matching conditions at $x = 0$ and x_e, namely, at $x = 0$:

$$\psi = \begin{cases} \Psi_I, & y_s \le y \le y_n \\ \Psi_I \dfrac{y}{y_s} & 0 \le y \le y_s \\ \Psi_I \dfrac{(1-y)}{(1-y_n)} - \dfrac{(y-y_n)}{(1-y_n)} & y_n \le y \le 1 \end{cases}, \tag{2.11a,b,c}$$

where Ψ_I is the, as yet, unknown value of the geostrophic streamfunction on the island at $x = 0$. While at $x = x_e$, the flow is chosen to leave the domain as a uniform flow in the interval $y_e \le y \le y_e + d_e$, so that at x_e

$$\psi = \begin{cases} 0 & 0 \le y \le y_e \\ -\dfrac{y - y_e}{d_e} & y_e \le y \le y_e + d_e \\ -1 & y_e + d_e \le y \le 1 \end{cases}. \tag{2.12a,b,c}$$

The representations in (2.11) are, at best, an approximation of the true solution, but if the gaps between the island and the channel boundary are small, they are adequate for our purposes. The numerical experiments in section 5, even for islands of small meridional extent, qualitatively verify these representations. The specification of (2.12) is an allowed choice. In fact, in most of the calculations to be performed, the parameters y_e and d_e are chosen such that the exit flow is also uniform in y. All the coefficients in (2.9a) and (2.9b) are then determined in terms of the island constant Ψ_I. To determine the island constant, an additional constraint, Kelvin's theorem, is required.

c. Kelvin's theorem

An important constraint on the geostrophic streamfunction is provided by Kelvin's theorem (e.g., Pedlosky et al. 1997). For the inviscid, adiabatic flow considered here, the circulation of velocity around the island is conserved. If it is initially zero, it must remain so. If an otherwise negligible bottom friction is considered, any nonzero circulation will eventually decay away to zero in the steady state. That condition will be applied in all cases (except one discussed in section 3) and requires that

$$\int_{y_s}^{y_n} \frac{\partial \varphi}{\partial x}(0_-, y)\, dy = \int_{y_s}^{y_n} \frac{\partial \varphi}{\partial x}(0_+, y)\, dy, \tag{2.13}$$

where the integral on the left-hand side is evaluated on the western side of the island, while the integral on the right-hand side is evaluated on the island's eastern side. Since the coefficients in the solution for φ depend on the island constant, the integral constraint in (2.13) will

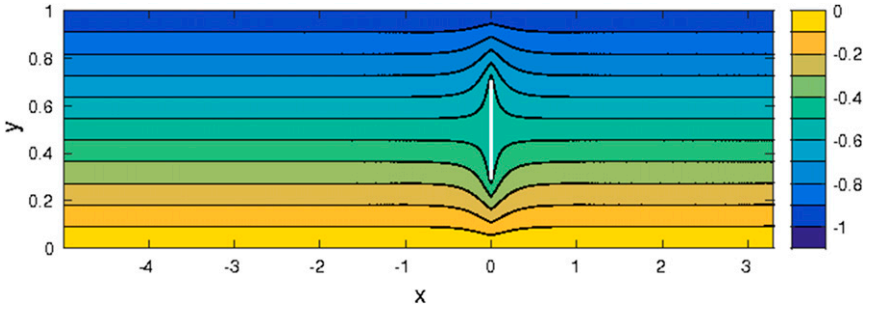

FIG. 3. The geostrophic streamfunction is shown for the supercritical flow $b = 0.5\pi^2$. The island is placed symmetrically in the channel. The island constant $\Psi_I = -0.5$, indicating that half of the impinging flow circulates around each end of the island.

determine Ψ_I, in terms of the magnitude of the velocity entering the channel and which is unity in our nondimensional variables. The calculation is algebraically lengthy, and the result is given in the appendix. It is not difficult to see from the result in the special case when the island is placed symmetrically about the channel's midpoint ($y = 1/2$), and the outflow also is symmetric about that midpoint, that the island constant is simply $\Psi_I = -0.5$, so that exactly half the oncoming flow transits the northern and southern paths around the islands. As shown in the following sections, breaking that symmetry leads to important variations in the transport paths. The parameter range $b < \pi^2$ (supercritical flow) will be investigated next.

3. Supercritical flow $b < \pi^2$

When $b < \pi^2$, the advective frequency, the mean zonal velocity, in our units unity, times the x wavenumber k is larger than the maximum magnitude of the intrinsic Rossby wave frequency $-bk/\pi^2$, so that no steady wave is possible. In that case, $J_w = 0$, and the solution involves only exponential behavior in x.

Figure 3 shows the flow for the supercritical flow $b = 0.5\pi^2$. The island is placed symmetrically about the midpoint in y of the channel. The island constant $\Psi_I = -0.5$, indicating that half of the impinging flow circulates around each end of the island. The fore–aft symmetry of the streamlines is a reflection of the inviscid dynamics and one would expect the presence of even a small amount of friction to alter the flow field, perhaps by separation, in the region to the east of the island. First, though, it is interesting to examine how the solution changes when the island is placed asymmetrically in the channel. In the symmetric case, just described, the dividing streamline intersects the midpoint of the island and is also the value of the island constant, for example, $\Psi_I = -0.5$. When the island is moved southward from the midline of the channel, we would expect Ψ_I to be smaller in magnitude to allow more of the oncoming fluid to flow north of the island. Since the oncoming flow is represented by the streamfunction $\psi = -y$, if the dividing streamline still were to occur at the midpoint of the island, the value of that streamline would be $\psi = (y_n + y_s)/2$. In Fig. 4, the island has been moved southward so that $y_s = 0.15$, $y_n = 0.55$, so that if dividing streamline had the value of the approaching flow's

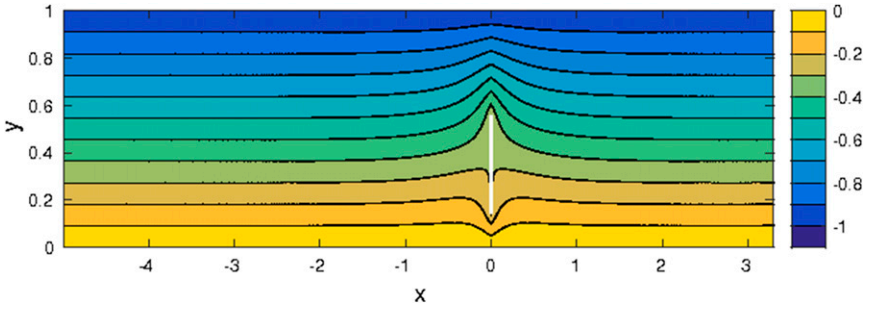

FIG. 4. As in Fig. 3, but the island is moved southward so that $y_n = 0.55$, $y_s = 0.15$. The island constant Ψ_I is -0.2777 and less than that would be expected if the flow divided evenly around the island.

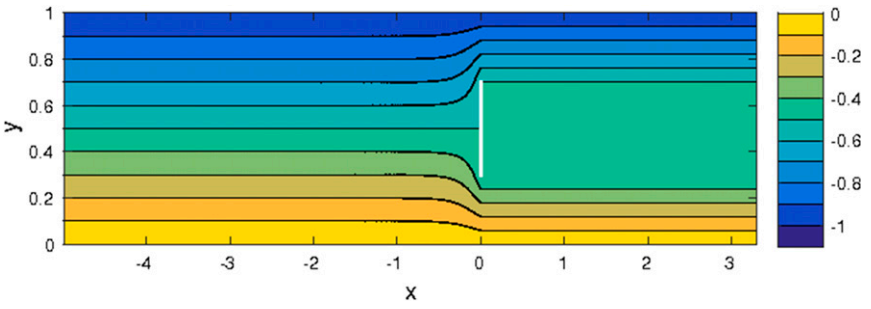

FIG. 5. The heuristic solution for separated, supercritical flow where all parameters are as in Fig. 3, but that the solution is given by (3.1), (3.2), and (3.3).

streamfunction at the midlatitude of the island, we would expect to have $\Psi_I = -0.35$; instead, the calculation outlined in the appendix yields $\Psi_I = -0.2777$. This implies that more flux flows around the northern end of the island than anticipated, clearly an effect of the closeness of the island to the southern boundary. Since the supercritical flow tends to remain zonal except in the vicinity of the island, the solution in this parameter range is insensitive to the longitudinal position of the island.

On the other hand, the numerical results described below in section 5 suggests that the flow is sensitive to relatively small values of friction leading to separation of the flow from the northern and southern tips of the island, leaving a stagnant bubble or wake east of the island. We can attempt a heuristic model of that flow by assuming that in the region east of the island the flow has separated, is strictly zonal, and is confined to the regions $0 \le y \le y_s$ and $y_n \le y \le 1$, while remaining at rest east of the island in $y_s \le y \le y_n$. In the region of the moving zonal flow, we will assume that the potential vorticity relation (2.3) holds on all streamlines, while accepting a jump in the zonal velocity at the boundaries between the stagnant and moving regions to represent the vorticity produced by the viscously generated separation. Thus, in $0 \le y \le y_s$, the solution will be

$$\psi = -y + (\Psi_I + y_s)\frac{\sinh b^{1/2} y}{\sinh b^{1/2} y_s}, \tag{3.1a}$$

which assures that the boundary conditions at $y = 0$ and $y = y_s$ are satisfied. For the northern branch of the current, the similar solution is

$$\psi = -y + (\Psi_I + y_n)\frac{\sinh b^{1/2}(y-1)}{\sinh b^{1/2}(y_n - 1)}, \tag{3.1b}$$

while $\psi = \Psi_I$ in the intervening y interval:

$$\psi = \Psi_I, \quad y_s \le y \le y_n. \tag{3.1c}$$

The solution in $x \le 0$ is given by the series

$$\psi = -y + \sum_{n=1} B_n \frac{\sinh \alpha_n (x - x_w)}{\sinh \alpha_n x_w} \sin n\pi y. \tag{3.2}$$

Here, the B_n are determined by matching ψ at $x = 0$, that is, to (3.1a), (3.1b), and (3.1c). The remaining unknown is the island constant Ψ_I. The original calculation is no longer pertinent in this separated solution. Instead, we imagine a circuit for the Kelvin integral that embraces the western edge of the island and then extends infinitely far to the east to close beyond the presence of the two shear layers at y_s and y_n. If the original contour contained no vorticity, the original value of the circulation was zero. If we insist that it remain so, the contribution to the Kelvin integral from the two shear layers will dominate the vorticity contained in the circuit and they must balance to leave a zero net contribution to the circulation. This yields a condition for Ψ_I, which with a little algebra results in

$$\Psi_I = -\frac{y_s \coth b^{1/2} y_s + y_n \coth b^{1/2}(1 - y_n)}{\coth b^{1/2} y_s + \coth b^{1/2}(1 - y_n)}. \tag{3.3}$$

Note that for the case where the island is placed symmetrically around the midpoint of the channel, (3.3) yields the simple result $\Psi_I = -(y_n + y_s)/2$, exactly as in the nonseparated flow. Figure 5 shows the solution for the same parameter values as in Fig. 3. Note that since the solution east of the island differs from the previous, nonseparated solution, the matching on $x = 0$ implies the solution west of the island will be slightly altered.

4. Subcritical flow

When $b \ge \pi^2$, the flow is subcritical and supports stationary Rossby waves with (nondimensional) wavenumber $k_j = (b - j^2\pi^2)^{1/2}$ for all j, such that the radicand is positive. When $\pi^2 < b < 4\pi^2$, only a single wave, corresponding to the gravest Fourier mode in y, is

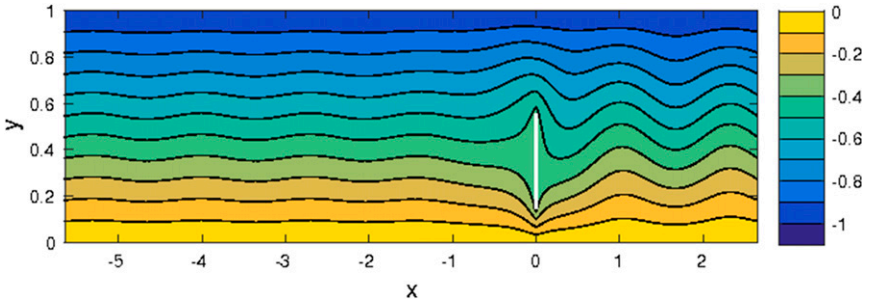

FIG. 6. The wavy flow around the same island as in Fig. 4, but for a subcritical value of $b = 3.35\pi^2$.

permitted. The nature of the flow depends critically on the geometry of the island. If the island is placed symmetrically about the midpoint of the channel, the disturbance to the flow by the island will have no projection on the $j = 1$ mode in (2.9a) and (2.9b), and the flow will look similar to the flow in Fig. 3. The higher modes in j, excited by the current's interaction with the island, will not radiate as Rossby waves. If the island is placed off center in the channel, as in Fig. 4, the flow will now be wavelike. As explained in section 2, the boundary condition at the eastern wall of the basin excites a global Rossby wave response. Figure 6 shows the calculated flow for the same geometric parameters as in Fig. 4 but now for a value of $b/\pi^2 = 3.35$. The wavy flow excited by the presence of the island yields an island constant $\Psi_I = -0.4114$, so that in this wavy case more of the flow passes to the south of the island than in the same configuration for the supercritical flow of Fig. 4. In fact, the island constant is sensitive to the phase of the wave at the island since it produces different angles of the impinging flow. Changing b changes the wavelength of the wave and the resulting change of wave phase at the island can strongly alter the island constant, that is, the partitioning of the flow pathways around the island. Figure 7a shows a solution for a smaller value of $b/\pi^2 = 2.5$ and hence a somewhat longer wavelength. The island constant is now -0.298 indicating more flow around the northern tip of the island. Similar alteration in flow path can also be achieved by changing the zonal position of the island. Note that the amplitude of the

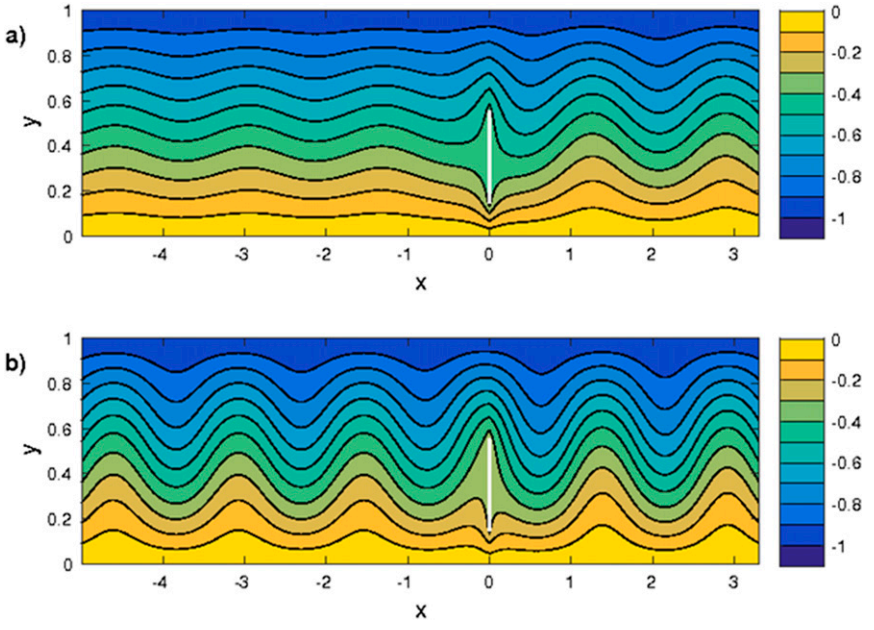

FIG. 7. (a) As in Fig. 6, but with a smaller value of $b = 2.5\pi^2$, yielding a slightly larger wavelength and a changed value of the island constant: $\Psi_I = -0.298$. This should be compared with Fig. 1. (b) A slightly larger value of $2.7\pi^2$ yields a more equal amplitude in the western region.

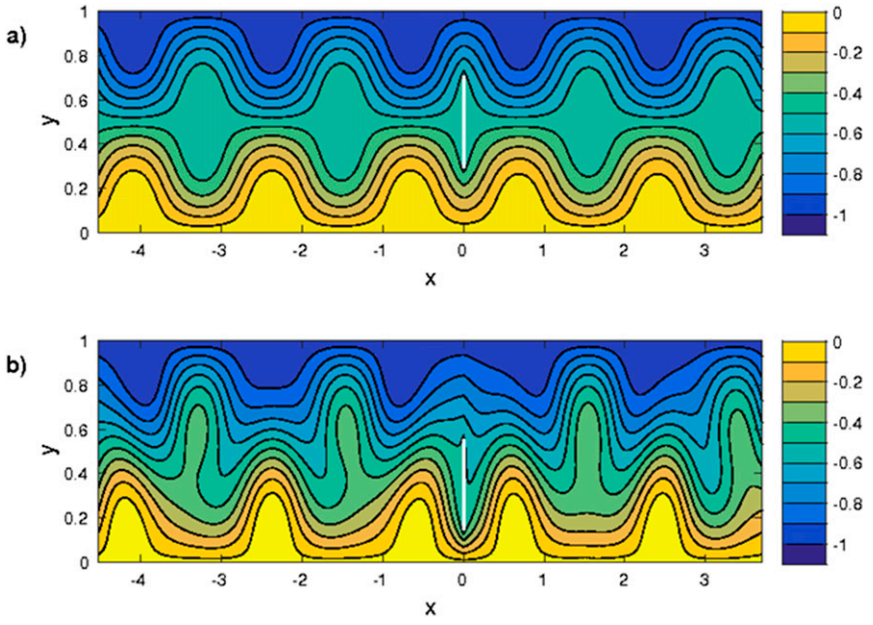

FIG. 8. The two wave case for $b = 5.35\pi^2$. (a) The solution for the symmetrically placed island showing that only the second cross-stream mode is excited. (b) The island is placed asymmetrically with regard to the channel midline, and both waves are now excited.

wave to the west of the island relative to the wave east of the island is also a function of b. Fig. 7b shows the solution for $2.7\pi^2$ for which the eastern and western amplitudes are essentially equal.

As b increases beyond $4\pi^2$, a second wave, with φ antisymmetric about the midline of the channel, becomes possible. In that range even the symmetrically placed island provokes a steady wave response as shown in Fig. 8. Figure 8a shows the solution for the symmetrically placed island and, as anticipated from our earlier discussion, only the $j = 2$ wave is excited by the island's presence. When the wave is moved off the centerline, as in Fig. 8b, both modes are excited and the solution becomes considerably more complex. In the former case, the island constant Ψ_I is very close to -0.5 as is expected. The asymmetric case, exciting both of the first two cross-stream modes, has an island constant $\Psi_I = -0.5247$, so that slightly more of the flow passes to the south of the island, even though the gap with the channel boundary is smaller. Finally, at the larger value of $b = 9.35\pi^2$, the flow allows three cross-stream waves, and all three are excited for an asymmetrically placed island. Figure 9 shows the complex flow the steady solution predicts. The island constant for this value of b is not much different from the single wave case of Fig. 6. As mentioned in the introduction, our interest is in values of b that are order unity, so much larger values of b than that already considered are less pertinent to the oceanographic case.

Based on the early work of Gill (1974), it is natural to expect the steady wave solutions would become

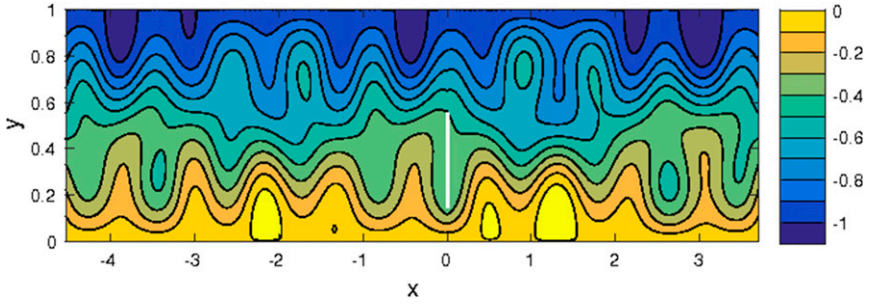

FIG. 9. The three-wave case. The island geometry is as in Fig. 7, but now $b = 9.35\pi^2$, so that the first three cross-stream modes are allowed.

unsteady to standard resonant interaction instabilities, and we will see in section 5 that the numerical solutions do, in fact, become time dependent for sufficiently low viscosity.

5. The numerical model and results

We test some of the basic ideas presented by the theory above with a shallow-water numerical model. The model represents a single moving layer of fluid overlying an infinitely thick, motionless deep layer. The model integrates the shallow-water primitive equations in the form

$$\frac{\partial \mathbf{V}}{\partial t} + (\zeta + f)\mathbf{k} \times \mathbf{V} = -\nabla\left(g'h + \frac{\mathbf{V}\cdot\mathbf{V}}{2}\right) + A_h\nabla^2\mathbf{V} - \gamma(\mathbf{V} - U\mathbf{i})$$

$$\frac{\partial h}{\partial t} + \nabla\cdot(\mathbf{V}h) = 0, \quad \mathbf{V} = (u, v), \tag{5.1a,b,c}$$

where $\zeta = (\partial v/\partial x) - (\partial u/\partial y)$ is the relative vorticity, A_h is a Laplacian viscosity coefficient, $f = f_0 + \beta y$ is the Coriolis parameter, g' is the reduced gravity, and $y = 0$ at the midlatitude of the channel. The model is configured in a periodic zonal channel with solid, free-slip walls at the northern and southern channel boundaries and at the island boundaries. The domain extends 4400 km in the zonal direction and 500 km in the meridional direction. Over most of the domain γ is zero and the model is unforced. Within the region $0 < x < 250$ km, $\gamma = 10^{-4}\,\mathrm{s}^{-1}$. This term relaxes the zonal velocity toward U and the meridional velocity toward zero and is the only forcing in the system. Inspection of the developing model fields indicates that waves are strongly damped in this region, effectively making the model channel not periodic but instead forced by an imposed inflow/outflow of uniform zonal velocity U. The results have been found to be insensitive to increasing the extent of the damping region or the details of the damping coefficient γ. A similar approach was used by Tansley and Marshall (2001). The equations are solved using centered finite differences on a 5-km grid with a third-order Adams–Bashforth time-stepping scheme. The model is started at rest and run for 20 yr, which is a sufficient period to arrive at a steady state or statistically steady state for time-dependent solutions. While the model is clearly very idealized compared to the real ocean, it does provide a means to determine whether the phenomenology identified with the quasigeostrophic theory above emerges in this dynamical framework that includes dissipation, primitive equation physics, time dependence, instabilities, and equatorial dynamics.

a. Supercritical flow

The supercritical flow condition is modeled with an imposed zonal velocity of $U = 1\,\mathrm{m\,s}^{-1}$ and $\beta = 2 \times 10^{-11}\,\mathrm{m}^{-1}\,\mathrm{s}^{-1}$, giving $b = 0.5\beta\pi^2$. For the midlatitude applications in this and the following subsection, $f_0 = 10^{-4}\,\mathrm{s}^{-1}$, the resting layer thickness $H_0 = 1000$ m, and the reduced gravity $g' = 0.05\,\mathrm{m\,s}^{-2}$, although the steady solutions are not strongly dependent on these parameter values. The Laplacian viscosity coefficient in this case is $500\,\mathrm{m}^2\,\mathrm{s}^{-1}$, which gives a grid cell Reynolds number of 10 and a flow Reynolds number based on the width of the channel of 1000. A narrow 10-km-wide island is placed at the midlatitude of the channel at longitude $x = 2250$ km. The mean streamfunction for this case is shown in Fig. 10a. The forcing region is located between $x = 0$ and the white line at $x = 250$ km. To the west of the island, the model streamfunction looks as expected from the theory. Far to the west of the island, the flow is zonal. As the island is approached, the flow develops an eastern boundary layer and flows to the north and south around the island. However, to the east of the island the flow looks much more like the heuristic solution for a separated flow. There is a nearly stagnant wake with weak recirculations that extend approximately 750 km to the east. Beyond that the streamfunction merges again to form a more zonal flow, similar to the upstream region, before entering the forcing region.

To the west of the island, the potential vorticity is dominated by the variation in layer thickness, which is an order of magnitude larger than the planetary vorticity gradient (Fig. 10b). This is why the gradient increases as the northern boundary is approached. The region to the east of the island shows two strong tongues of high and low potential vorticity extending off the southern and northern tips of the island and into the region of weak flow behind the island. There is also a source of high potential vorticity along the northern boundary just to the east of the island. Even though the model has free-slip boundary conditions, there is still a diffusive relative vorticity flux through the boundary. This is because $u_y = 0$ at the northern and southern boundaries, but u_{yy} is not equal to zero. It is these boundary sources of potential vorticity that cause the numerical model to differ from the theory, which imposes conservation of potential vorticity. Although free-slip boundary conditions are not equivalent to a condition of no flux of relative vorticity, some of this production is likely related to the numerical implementation of the free-slip boundary condition at the corners of the island (see Adcroft and Marshall 1998).

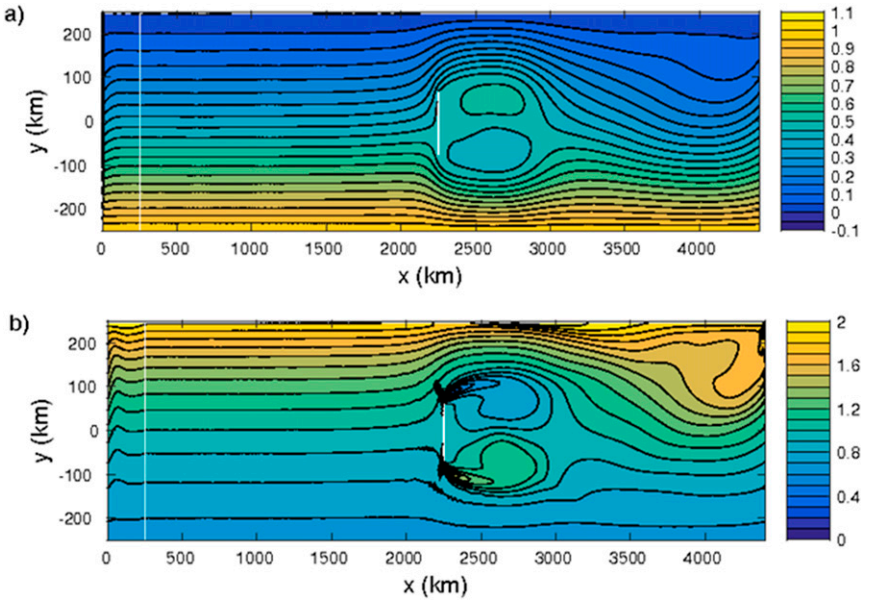

FIG. 10. (a) The nondimensional streamfunction pattern from the shallow-water model for the supercritical flow, $b = 0.5\beta\pi^2$, $A_h = 500\,\mathrm{m^2\,s^{-1}}$. (b) The field of potential vorticity scaled by $f_0/h_0 = 10^{-7}\,\mathrm{m^{-1}\,s^{-1}}$. The flow most closely resembles the heuristic separated flow of Fig. 5. The white line at $x = 250$ km indicates the limit of the region where the γ term in the momentum equation acts to restore the flow to a purely zonal velocity.

b. *Subcritical flow*

When the zonal flow is reduced to $U = 0.15\,\mathrm{m\,s^{-1}}$, the parameter $b = 3.35\pi^2$ and the theory indicates that the flow will support stationary mode-1 waves, provided that the island is not symmetric in latitude, in which case the wave, though allowed, is not provoked by the island. (This weaker flow allows for a reduction in the viscosity coefficient to $250\,\mathrm{m^2\,s^{-1}}$.) For an island that is offset to the south, the model indeed produces a standing wave pattern that is very similar to that predicted by the theory (Fig. 11a). The wave amplitude is larger to the east of the island than it is to the west of the island, consistent with Fig. 6. The relative amplitude east and west of the island in the model depends on b, as in the theory (cf. Figs. 1 and 11). One difference with the theory is that the amplitude of the wave, particularly to the east of the island, decreases away from the island over a distance of several wavelengths. This is likely due to the lateral viscosity in the model. Potential vorticity is nearly conserved over most of the domain (Fig. 11b), as assumed in the theory. The island still produces tongues of anomalous potential vorticity extending eastward from the tips of the island, but they are confined more closely to the island than in the supercritical case.

The case for which the first two Rossby modes are allowed with a centrally located island is considered for $b = 7.6\pi^2$ ($\beta = 3 \times 10^{-11}\,\mathrm{m^{-1}\,s^{-1}}$; $U = 0.1\,\mathrm{m\,s^{-1}}$) in Fig. 12. This does excite only the mode-2 wave, as expected, but the amplitude varies strongly in the zonal direction. This flow is qualitatively similar to that found by Tansley and Marshall (2001) for their moderate Re calculation with $b = 7.5$ and a smaller, circular island. The meanders are largest just to the east of the island and decrease toward the east, similar to the mode-1 case. However, the amplitude is much weaker to the west of the island and also shows a suggestion of an exponentially decaying mode-2 wave to the west of the island whose cause we find puzzling but may be related to the upstream blocking for large b discussed by Page and Johnson (1990) and Tansley and Marshall (2001). The resulting negative anomaly in the south and positive anomaly in the north causes a region of reduced zonal flow within the latitude band of the island. Close examination of the streamfunction and potential vorticity near the western side of the island reveals a viscous boundary layer of width $O(20)$ km, consistent with a Munk layer of thickness $\delta_M = (A_h/\beta)^{1/3}$.

An identical calculation with the horizontal viscosity reduced to $100\,\mathrm{m^2\,s^{-1}}$ produces a similar mean circulation, but the viscous boundary layer on the western side of the island is reduced and the amplitude of the mode-2 wave is slightly larger to the west of the island, in closer agreement with the inviscid theory. The solutions also become strongly time dependent, particularly to the east

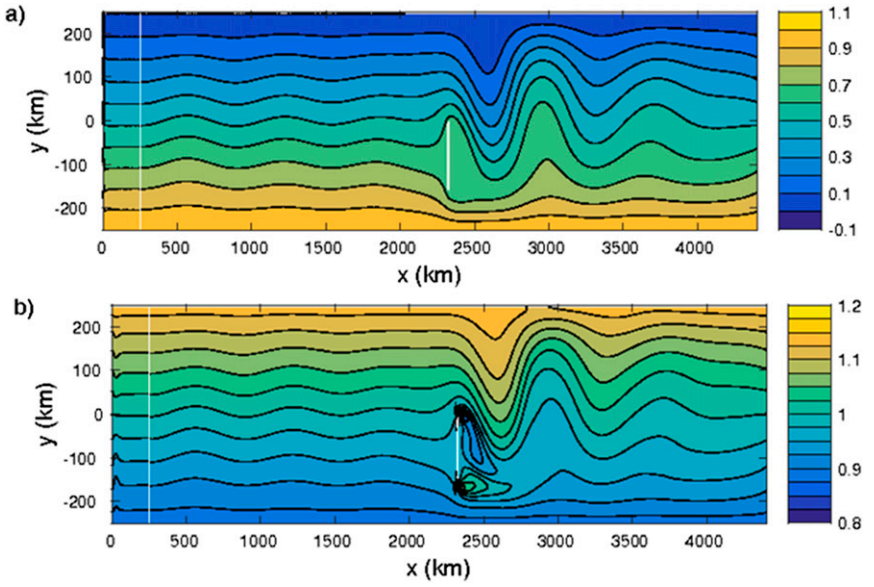

FIG. 11. The numerical solution for the subcritical flow with $b = 3.35\pi^2$, $A_h = 250\,\mathrm{m^2\,s^{-1}}$, as in Fig. 6. (a) Streamfunction pattern. (b) The potential vorticity. Note the viscously produced but confined tongues of anomalous potential vorticity at the tips of the island.

of the island. An example of the synoptic streamfunction and potential vorticity are shown in Fig. 13. Complex empirical orthogonal functions show that the perturbations are dominated by an $O(1)$ mode-2 meridional structure, although there is also significant energy in mode 1. The mode-2 features propagate westward at approximately $3\,\mathrm{cm\,s^{-1}}$ with maximum amplitude in the eastern basin. The mode-1 features are stronger in the western basin, although the propagation is less clear.

c. *Equatorial application*

Part of the motivation for this study, as mentioned in the introduction, is the interaction of the Equatorial Undercurrent with the Galapagos Islands. Naturally, the

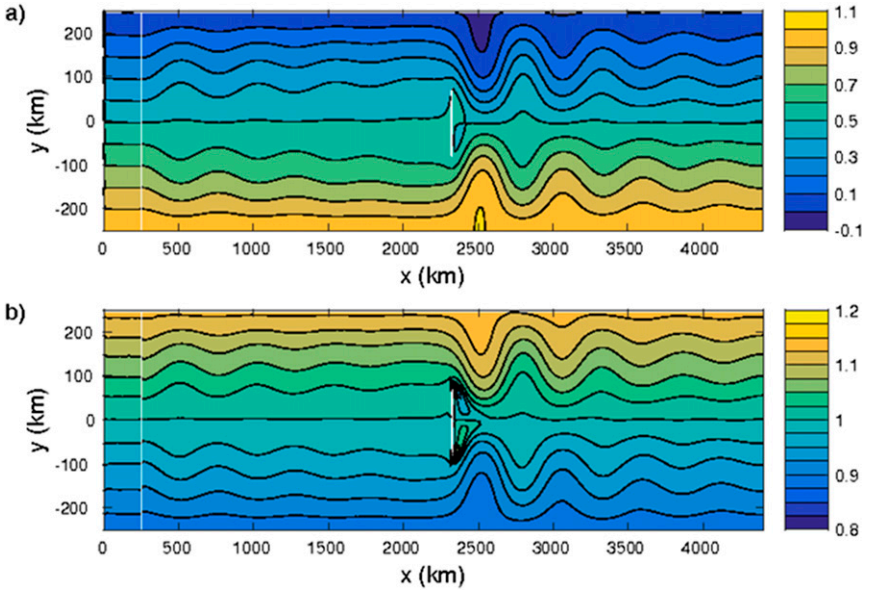

FIG. 12. Subcritical flow with $b = 7.6\pi^2$, $A_h = 250\,\mathrm{m^2\,s^{-1}}$. (a) Streamfunction pattern showing the production of mode 2 for the symmetrically placed island. (b) The potential vorticity field.

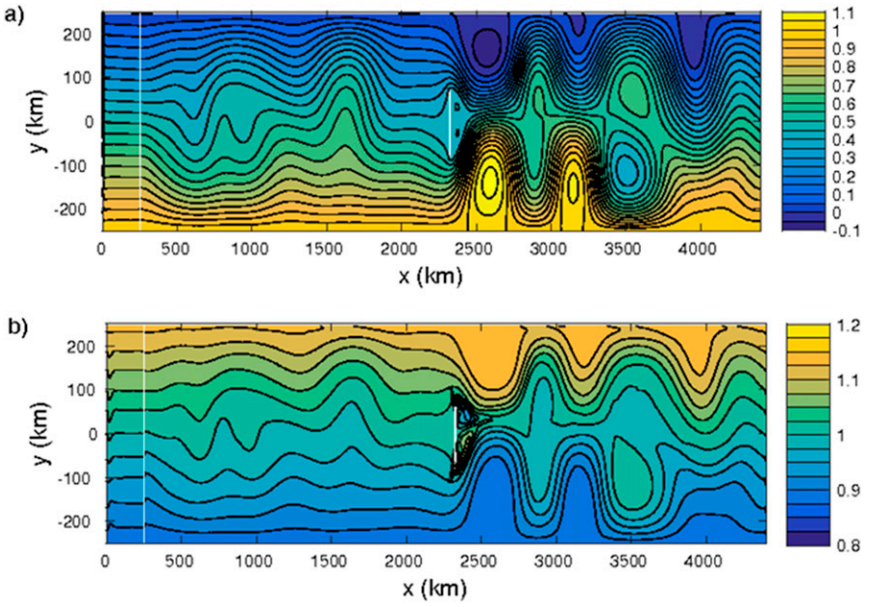

FIG. 13. The subcritical case as in Fig. 12, but now the lateral viscosity A_h is reduced to $100\,\mathrm{m^2\,s^{-1}}$. The flow is now time dependent; this is day 4800. See text for discussion.

quasigeostrophic model used in sections 3 and 4 to this point is clearly not valid at the equator. However, there are reasons to believe that the steady model described in those previous two sections may be more relevant than expected at first sight. We will show this in detail in the discussion of the extension of the numerical work in sections 5a and 5b to nonquasigeostrophic theory, so we can consider the flow in the equatorial domain, but we pause here to make a case for its qualitative pertinence, at least for small islands, where smallness has to be defined. In our numerical model, the steady-state flow possesses a streamfunction for the volume flux. With h as the layer thickness, the continuity equation is satisfied by

$$h\mathbf{V} = \mathbf{k} \times \nabla\psi. \tag{5.2}$$

If the inflow at the western boundary of our channel has a uniform inflow volume flux M, then at $x = x_w$,

$$\psi = -My. \tag{5.3}$$

Since we specify that at the inflow there is no relative vorticity and the fluid is in geostrophic balance, it is easy to show that for the inflow

$$h^2 = h_0^2 - \frac{M\beta y^2}{g'} = h_0^2 - \frac{\beta\psi^2}{Mg'}, \tag{5.4}$$

where h_0 is the constant thickness at $y = 0$, the center of the equatorial channel. If potential vorticity is conserved so that

$$q = \frac{\zeta + \beta y}{h} = Q(\psi), \tag{5.5}$$

it follows, using (5.4), that

$$Q(\psi) = \frac{\zeta + \beta y}{h} = \frac{\left(\frac{\psi_x}{h}\right)_x + \left(\frac{\psi_y}{h}\right)_y + \beta y}{h} = \frac{\beta\psi/M}{\left(h_0^2 - \frac{\beta\psi^2}{Mg'}\right)^{1/2}}. \tag{5.6}$$

The right-hand side of (5.6) bears a strong resemblance to (2.3) except for the dependence of the denominator of the final term in (5.6) on the streamfunction. If ℓ is the horizontal scale of the motion (and it could be smaller than the channel width), the relative size of that term to h_0^2 can be shown to be of the order of $(\ell/L_{\mathrm{eq}})^4(\delta_I/\ell)^2$, where the equatorial deformation radius is defined as $L_{\mathrm{eq}} = (g'h_0/\beta^2)^{1/4}$, while the inertial boundary layer parameter $\delta_I = (U/\beta)^{1/2}$. Hence, for small enough islands such that the scale is much less than the equatorial deformation radius, (5.6) will strongly resemble the quasigeostrophic model. We do not mean to imply that the quasigeostrophic model is quantitatively accurate at the equator, only that there is strong reason to believe in the expectation of a qualitative similarity for the steady solutions. The numerical results we discuss now verify that expectation.

The shallow-water model is now configured for an equatorial domain. The Coriolis parameter f_0 is set to

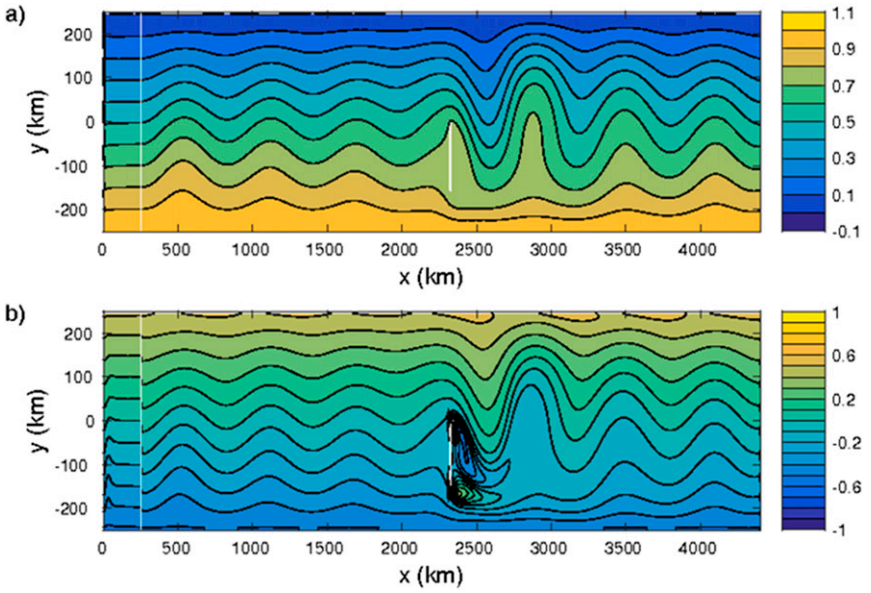

FIG. 14. The mean streamfunction and potential vorticity for the subcritical case $b = 3.35\pi^2$, as in Fig. 11, but set on the equator. In (b), the potential vorticity is scaled by $\beta L/h_0$.

zero, the resting layer thickness H_0 is reduced to 200 m, and the reduced gravity $g' = 0.01\,\mathrm{m\,s^{-1}}$. This gives a Kelvin wave speed of $1.4\,\mathrm{m\,s^{-1}}$ and an equatorial deformation radius of 265 km. For the case shown below, $U = 0.15\,\mathrm{m\,s^{-1}}$, the inertial boundary layer thickness $\delta_I = 86$ km, and we take $\ell = 150$ km to be the island extent. The scaling parameter $(\ell/L_{\mathrm{eq}})^4(\delta_I/\ell)^2$, which measures the relative variation of the layer thickness with respect to its mean value for this calculation, is 0.03, and so this configuration falls into the small island regime for which the midlatitude theory should remain applicable.

The mean circulation for the supercritical and subcritical cases in this equatorial domain looks very similar to that found for the midlatitude domain. As an example, the mean streamfunction and potential vorticity for the subcritical case with $b = 3.35\pi^2$ is shown in Fig. 14 (cf. with Fig. 11). We see a very similar standing wave pattern with larger-amplitude meanders to the east and smaller-amplitude meanders to the west of the island. The waves to the west of the island are similar in wavelength to the midlatitude case but have larger amplitude, particularly as the island is approached. Similar tongues of potential vorticity extend from the tips of the island, although the background potential vorticity changes sign as the equator is crossed. Kelvin waves are excited during the spinup of the calculation, but they propagate rapidly eastward into the forcing region, where they are damped. After this initial adjustment there is very little excitation of the higher-frequency equatorial waves, and the balance between mean advection and westward propagation of the Rossby waves dominates the circulation, as expected from the discussion leading to (5.6).

6. Summary and discussion

We have used a midlatitude model to discuss the interaction of an eastward-flowing zonal current with an island that lies athwart the stream. The problem is suggested by the interaction of the Equatorial Undercurrent with the Galapagos Islands in the Pacific and our use of midlatitude dynamics allows us to concentrate on the issue of the supercriticality of the flow with respect to Rossby wave propagation alone. This reduced problem, and even in its simplest one-layer version, contains unexpectedly subtle dynamics. In the supercritical case, where $b = \beta L^2/U < \pi^2$, a completely inviscid and adiabatic model that conserves potential vorticity naturally leads to flow patterns that are symmetric upstream and downstream of the island. We have shown, using our numerical model, that the presence of friction breaks that symmetry and produces a downstream wake that we have heuristically modeled with our analytical model. The subcritical case for which b is greater than π^2, introduces a globally wavy nature to the flow. The amplitude and the phase of the wave at the island depends on the magnitude of b, the position of the island relative to the inflow and outflow boundaries, as well as the meridional placement of the island in its channel. That being the case, generally, the value of the streamfunction on the island and hence the portion of

the oncoming flow that flows to the north or south of the island depend on each of these parameters. Our numerical model suggests that these results may qualitatively be valid at the equator.

It will be of interest to extend the problem in several directions. A model that allows cross-interface flow and upwelling at the island can examine the question of whether the oncoming flow completely circumvents the island or whether a portion is exported to a neighboring layer and returned to the west. Similarly, moving the dynamics to the equator and using a current whose latitudinal structure is more realistic, that is, abandoning the channel model in favor of an equatorial current with a maximum at the equator, will be necessary to discuss a realistic equatorial application. These are problems for future study.

Acknowledgments. M. Spall's research was supported by the National Science Foundation Grant OCE-0959381. We thank two anonymous reviewers and David Marshall for their helpful comments and suggestions.

APPENDIX

The Island Constant

Upon application of the boundary conditions (2.6), (2.11), and (2.12), we obtain the following result for the island constant Ψ_I:

$$\Psi_I = Q/P, \tag{A.1}$$

where

$$Q = -\left[2\sum_{j=J_w+1}^{J_{\max}} \frac{\alpha_j}{(j\pi)^3}\frac{\sin j\pi y_n}{d_n}\right](\cos j\pi y_n - \cos j\pi y_s) - \sum_{j=1}^{J_w}\frac{k_j}{(j\pi)^3}\frac{\sin j\pi y_n}{d_n}(\cot k_j x_e - \cot k_j x_w)$$
$$- \sum_{j=1}^{J_w}\frac{k_j}{(j\pi)^3}[\sin j\pi(y_e + de) - \sin j\pi y_e]\frac{(\cos j\pi y_n - \cos j\pi y_s)}{\sin k_j x_e}, \quad \text{and} \tag{A.2}$$

$$P = 2\sum_{j=J_w+1}^{J_{\max}} \frac{\alpha_j}{(j\pi)^3} F_j(\cos j\pi y_s - \cos j\pi y_n) + \sum_{j=1}^{J_w}\frac{k_j}{(j\pi)^3}(\cot k_j x_e - \cot k_j x_w)F_j(\cos j\pi y_s - \cos j\pi y_n), \tag{A.3}$$

and with $d_n = 1 - y_n$, $d_s = y_s$,

$$F_j = \frac{\sin j\pi y_s}{d_s} + \frac{\sin j\pi y_n}{d_n}. \tag{A.4}$$

REFERENCES

Adcroft, A., and D. Marshall, 1998: How slippery are piecewise-constant coastlines in ocean models? *Tellus*, **50A**, 95–108, doi:10.1034/j.1600-0870.1998.00007.x.

Charney, J. G., 1960: Non-linear theory of a wind-driven homogeneous layer near the equator. *Deep-Sea Res.*, **6**, 303–310, doi:10.1016/0146-6313(59)90089-9.

Gill, A. E., 1974: The stability of planetary waves on an infinite beta-plane. *Geophys. Fluid Dyn.*, **6**, 29–47, doi:10.1080/03091927409365786.

Karnauskas, K. B., R. Murtugudde, and A. J. Busalacchi, 2007: The effect of the Galápagos Islands on the equatorial Pacific cold tongue. *J. Phys. Oceanogr.*, **37**, 1266–1281, doi:10.1175/JPO3048.1.

——, ——, and ——, 2010: Observing the Galápagos–EUC interactions: Insights and challenges. *J. Phys. Oceanogr.*, **40**, 2768–2777, doi:10.1175/2010JPO4461.1.

Page, M. A., and E. R. Johnson, 1990: Flow past cylindrical obstacles on a beta-plane. *J. Fluid Mech.*, **221**, 349–382, doi:10.1017/S0022112090003597.

Pedlosky, J., 1987a: An inertial theory of the Equatorial Undercurrent. *J. Phys. Oceanogr.*, **17**, 1978–1985, doi:10.1175/1520-0485(1987)017<1978:AITOTE>2.0.CO;2.

——, 1987b: *Geophysical Fluid Dynamics.* 2nd ed. Springer-Verlag, 710 pp.

——, L. J. Pratt, M. A. Spall, and K. R. Helfrich, 1997: Circulation around islands and ridges. *J. Mar. Res.*, **55**, 1199–1251, doi:10.1357/0022240973224085.

Tansley, C. E., and D. P. Marshall, 2001: Flow past a cylinder on a β plane, with application to Gulf Stream separation and the Antarctic Circumpolar Current. *J. Phys. Oceanogr.*, **31**, 3274–3283, doi:10.1175/1520-0485(2001)031<3274:FPACOA>2.0.CO;2.